Journal of Biomechanics ∎ (∎∎∎∎) ∎∎∎–∎∎∎

Contents lists available at ScienceDirect

Journal of Biomechanics

journal homepage: www.elsevier.com/locate/jbiomech
www.JBiomech.com

Biomechanical properties of native and tissue engineered heart valve constructs

Anwarul Hasan [a,b], Kim Ragaert [c], Wojciech Swieszkowski [d], Šeila Selimović [a,b], Arghya Paul [a,b,f], Gulden Camci-Unal [a,b], Mohammad R.K. Mofrad [e], Ali Khademhosseini [a,b,f,g,*]

[a] Center for Biomedical Engineering, Department of Medicine, Brigham and Women's Hospital, Harvard Medical School, Cambridge, MA 02139, USA
[b] Harvard-MIT Division of Health Sciences and Technology, Massachusetts Institute of Technology, Cambridge, MA 02139, USA
[c] CPMT Group, Department of Materials Science & Engineering, Faculty of Engineering & Architecture, Ghent University, Belgium
[d] Faculty of Materials Science and Engineering, Warsaw University of Technology, 02-507 Warsaw, Poland
[e] Departments of Bioengineering and Mechanical Engineering, University of California, Berkeley, CA, USA
[f] Wyss Institute for Biologically Inspired Engineering, Harvard University, Boston, MA 02115, USA
[g] World Premier International – Advanced Institute for Materials Research (WPI-AIMR), Tohoku University, Sendai 980-8577, Japan

ARTICLE INFO

Article history:
Accepted 10 September 2013

Keywords:
Aortic and pulmonary heart valves
Tissue engineering
Mechanical properties
Biomechanics

ABSTRACT

Due to the increasing number of heart valve diseases, there is an urgent clinical need for off-the-shelf tissue engineered heart valves. While significant progress has been made toward improving the design and performance of both mechanical and tissue engineered heart valves (TEHVs), a human implantable, functional, and viable TEHV has remained elusive. In animal studies so far, the implanted TEHVs have failed to survive more than a few months after transplantation due to insufficient mechanical properties. Therefore, the success of future heart valve tissue engineering approaches depends on the ability of the TEHV to mimic and maintain the functional and mechanical properties of the native heart valves. However, aside from some tensile quasistatic data and flexural or bending properties, detailed mechanical properties such as dynamic fatigue, creep behavior, and viscoelastic properties of heart valves are still poorly understood. The need for better understanding and more detailed characterization of mechanical properties of tissue engineered, as well as native heart valve constructs is thus evident. In the current review we aim to present an overview of the current understanding of the mechanical properties of human and common animal model heart valves. The relevant data on both native and tissue engineered heart valve constructs have been compiled and analyzed to help in defining the target ranges for mechanical properties of TEHV constructs, particularly for the aortic and the pulmonary valves. We conclude with a summary of perspectives on the future work on better understanding of the mechanical properties of TEHV constructs.

1. Introduction

Heart valve diseases are among the leading causes of death (Simionescu et al., 2012). Each year more than 290,000 patients go through valve replacement surgeries worldwide, and this number is projected to reach 850,000 by the year 2050, as the average age of the population increases (Loftin et al., 2011; Yacoub and Takkenberg, 2005). While currently the preferred method of treating heart valve patients is to repair the diseased valves, in case of severe heart diseases a large number of valves cannot be repaired and therefore require replacement (Yacoub and Takkenberg, 2005). There are two types of artificial heart valves clinically available for replacement: mechanical and bioprosthetic valves (Lim and Boughner, 1976). A major disadvantage of both types is that they do not allow for somatic growth or remodeling after implantation. This is a major drawback especially for children, whose valves must grow over time. Otherwise, as these patients grow, they will require replacement with a larger size valve every few years. Besides, mechanical valves are prone to infection, inflammation and thrombosis, while bioprosthetic valves experience calcification which has both a thickening and a stiffening effect on the valve cusps, eventually leading to insufficient valve closure and leakage (Sabbah et al., 1986). Tissue engineering offers immense potential to generate the suitable viable valve replacement method (Durst et al., 2011; Du et al.,

* Corresponding author at: Center for Biomedical Engineering, Department of Medicine, Brigham and Women's Hospital, Harvard Medical School, Cambridge, MA 02139, USA. Tel.: +1 617 768 8395.
E-mail address: alik@rics.bwh.harvard.edu (A. Khademhosseini).

0021-9290/$ - see front matter © 2013 Elsevier Ltd. All rights reserved.
http://dx.doi.org/10.1016/j.jbiomech.2013.09.023

2008; Flanagan and Pandit, 2003; Gauvin et al., 2011; Khademhosseini et al., 2009; Vesely, 2005). The approach of tissue engineering is to generate implantable tissues by encapsulating or seeding cells in biodegradable scaffolds, culturing the cell seeded constructs under appropriate environmental cues in bioreactors to induce tissue formation, and implanting these pre-conditioned constructs *in vivo* (Hasan et al., in press).

Tissue engineered implants are expected to gradually acquire the structural and mechanical characteristics of the native tissues through remodeling, repair, and growth upon implantation. Hence, the tissue engineered constructs do not have to be exact replicas of the native tissues at the time of implantation. In case of heart valves, however, the ability of the engineered construct to provide sufficient mechanical function immediately upon implantation is crucial for the survival of the patient. Therefore, successful application of tissue engineering in the development of heart valves will require that the tissues engineered constructs exhibit and maintain the mechanical properties similar to those of native valves (Driessen et al., 2007). However, because of the limited availability of fresh heart valves and proper test conditions, there have been a limited number of studies investigating the biomechanical properties of human aortic and pulmonary heart valves (Balguid et al., 2007; Clark, 1973; Martin and Sun, 2012; Stradins et al., 2004).

The current review is intended to present a comprehensive summary of the experimental data on biomechanical properties of human and animal native heart valves as well as those of the TEHV constructs. We focus on the pulmonary and aortic heart valves as these two types experience high mechanical stresses, and their semilunar tri-leaflet structure, composition, size, and direction of blood flow (outward) from the heart are so similar that one of them is often replaced by the other. The review also reveals the inadequacy of available data for mechanical properties in the literature and points toward the need for more experimental investigation of dynamic mechanical properties of heart valve constructs.

2. Structure and composition of aortic and pulmonary heart valves

The tricuspid, pulmonary, mitral and aortic valves lie on a common plane in the heart, termed as valvular basal plane as shown in Fig. 1(ai). The tricuspid and mitral valves regulate the inflow of blood to the right and left atrium respectively. The pulmonary valve regulates the outward flow from right ventricle of the heart to the pulmonary artery while the aortic valve controls the flow to the aorta from the left ventricle. Blood flows from the aorta to the major arteries, small arteries, arterioles, capillaries, venioles, and veins throughout the body, finally returning through the tricuspid valve to the top right chamber of the heart. The aortic and pulmonary valves possess similar structures. Both of them are composed of three semilunar leaflets or cusps along with their respective sinus complexes called valve roots. Figs. 1a(ii)–(iv) present some native and tissue engineered porcine and human pulmonary and aortic heart valves. The valve leaflets are composed of four main components, namely the hinge (also named as the commissural region), the belly, the lannula with the noduli of Arantii, and the coapting surface (Misfeld and Sievers, 2007). The cross-sectional structure of the leaflets is a thin, flexible, trilayered structure that can be divided into three sublayers, namely, fibrosa, spongiosa, and ventricularis (Cox, 2009) as shown in Fig. 1 (b) and (c).

Fibrosa, the thickest of the three layers, is primarily comprised of a highly dense network of corrugated collagen type-I fibers, which are arranged mostly in longitudinal direction and to a lesser degree in radial direction as well (Misfeld and Sievers, 2007). The radial fibers are much more crimped compared to the longitudinal ones. The elastin in the fibrosa forms a highly organized network of filaments stretching radially from the central region to the line of attachment of the leaflet. The walls of these tubes contain dense elastin sheets, which surround the collagen fiber bundles. Elastin, a highly elastic protein, stores energy during the loading of the valve and releases it to the collagen during unloading, thus allowing the valve to return to its resting position (Adham et al., 1996; Isenberg et al., 2006). Spongiosa, the sandwiched middle layer, consists of highly hydrated glycosaminoglycans (GAGs) and proteoglycans (PGs) as well as some loosely arranged collagen and elastin. It acts as a buffer zone between fibrosa and ventricularis and enables shearing between the two layers during loading and unloading. It absorbs the load and transfers it to the elastic aortic wall, resulting in minimum stress on the leaflet itself. Ventricularis, the thinnest of the three layers, consists of a collagen fiber network and elastin sheets – becoming a fibrous mesh at the edges – longitudinally arranged as shown in Figs. 1(d) and (e). In terms of functionality, the fibrosa acts as the main load-bearing layer, the spongiosa work as a cushion, lubricating the interface between spongiosa and ventricularis layers, while the ventricularis assists in reducing the large radial strains during the high blood flow over the valves when they are fully opened. The tri-layered structure of the valves ensures the high tensile strength for resisting the high transvalvular pressures and the low flexural stiffness as required for normal opening of the valve (Sacks et al., 1998). All leaflet layers consist of a network of collagen and elastin fibers saturated with fluids. The microstructural composition of the heart valve tissue determines its non-linear stress–strain characteristics. At very small initial strain, the wavy collagenous and elastin fibers can be stretched with relatively small forces, whereas straight fibers are much stiffer. This explains the dramatic increase in stress required to stretch the tissue. Besides, water comprises about 60–70% of the collagenous tissue by weight, and the water molecules are tightly bound to the fibrous network, which makes the tissue almost incompressible. It is likely that the water content contributes to viscous response of tissues. The annulus of the heart valves consists of dense collagenous meshwork (Misfeld and Sievers, 2007) in which elastic and collagenous fibrils are present. The collagenous fibers of the intermediate layer are oriented radially (Misfeld and Sievers, 2007), as shown schematically in Fig. 1(e).

The main cells present in heart valves include (i) the interstitial cells and (ii) the endothelial cells. The valvular interstitial cells are phenotypically of smooth muscle cells, cardiac muscle cells or the fibroblasts cell types (Brand et al., 2006), but they mostly exhibit the characteristics of smooth muscle cells and myofibroblast cells. They are also responsible for the production of glycosaminoglycans (GAGs), which can retain water and are believed to be responsible for the damping of mechanical forces and the viscoelastic properties of the valve (Sacks et al., 2009). The surface of the leaflets is covered with a continuous layer of valvular endothelial cells. The alignment of the endothelial cells is orthogonal, not parallel, to the blood flow. Some nerve cells are also present to varying degrees in different valves (Flanagan and Pandit, 2003).

3. Physiological forces and biomechanics of heart valves

Enforcing and controlling a unidirectional blood flow during cardiac cycle is the primary function of heart valves. They are considered as passive tissues directed by the inertial forces of the blood flow. The heart valves operate under a complex cyclic tensile–shear–flexural loading environment of tremendously high mechanical demand with a cyclic loading of about 30 million times

Please cite this article as: Hasan, A., et al., Biomechanical properties of native and tissue engineered heart valve constructs. Journal of Biomechanics (2013), http://dx.doi.org/10.1016/j.jbiomech.2013.09.023

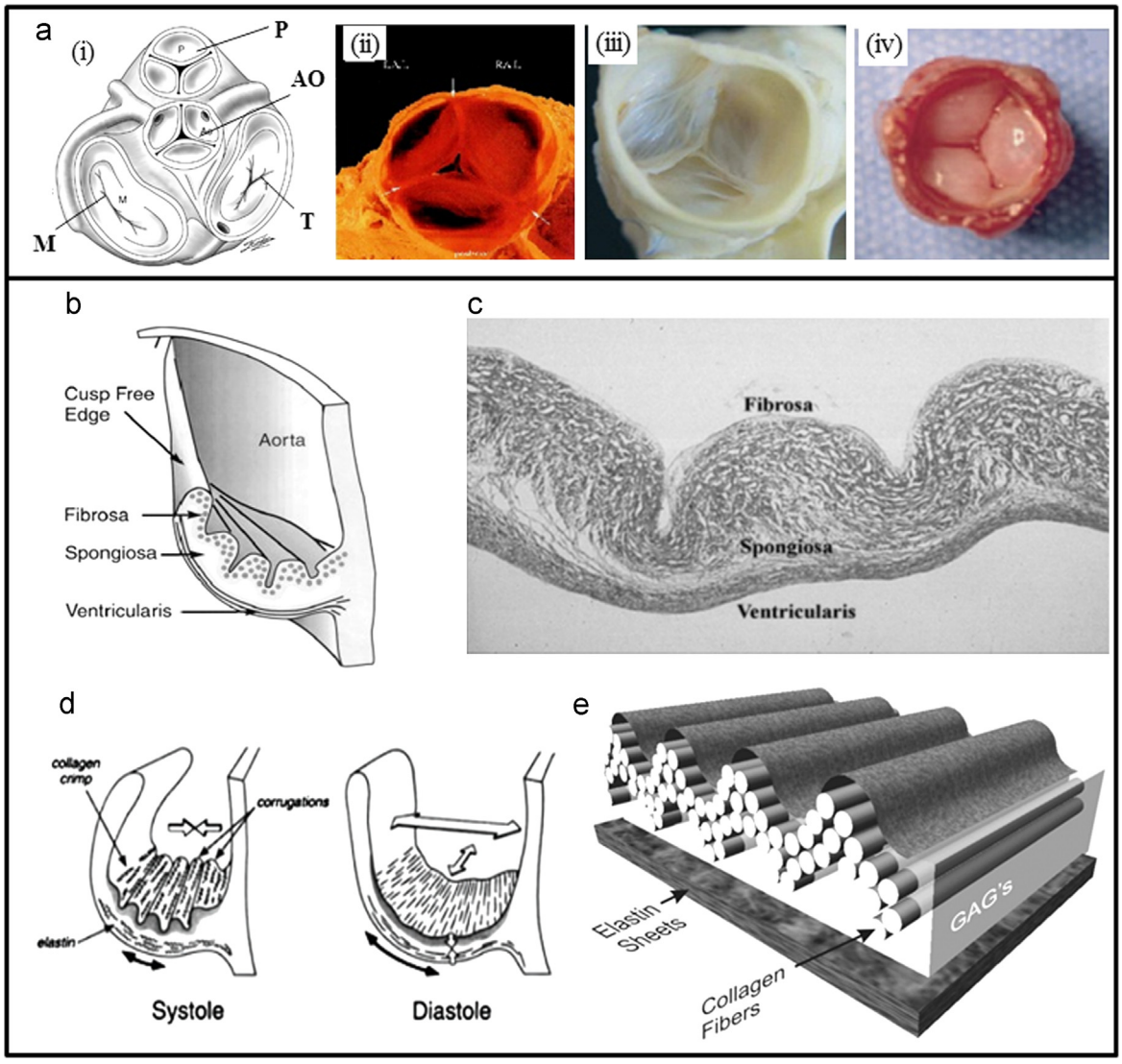

Fig. 1. Heart valve structure and composition: (a) structure of heart valves, (i) schematics of the 2D position of the four valves on valvular basal plane of heart where P: pulmonary valve, AO: aortic valve, M: mitral valve, and T: tricuspid valve, (ii–iv) some native and tissue engineered heart valves: (ii) porcine pulmonary heart valve, (iii) decellularized porcine aortic heart valve, and (iv) tissue engineered human heart valve. (b–e) Composition of the heart valves: (b) schematic of the cross section of an aortic valve leaflet, (c) histology of the cross section of a valve leaflet showing the three main layers, fibrosa, spongiosa and ventricularis, (d) schematic of the elastin and collagen microstructure in different layers during systolic and diastolic cycles, and (e) arrangement of collagen fibers as well as distribution of elastin and GAG's.
Figures adapted and reprinted from Butcher et al. (2011), Latremouille and Lintz (2005), McAlpine (1975), Misfeld and Sievers (2007), Sutherland et al. (2005), Carew et al. (2003), and Vesely (1998), (2005), with permissions from the Royal Society of Chemistry and Elsevier Science.

Table 1
Transvalvular pressures for human and bovine heart valves. with permission from American physiological society.
Reprinted from Aldous et al. (2009)

	Transvalvular pressure (mmHg)		Basis for bovine values (mmHg)	Reference
	Human	Bovine		
Mitral valve	120	144	Systolic LV pressure=150	Doyle et al. (1960)
			Systolic LA pressure=6	Kuida et al. (1961)
Aortic valve	80	92.4	Diastolic atrial pressure=92.4	Amory et al. (1992)
			Diastolic LV pressure=0	Doyle et al. (1960)
Tricuspid valve	25	27.2	Systolic RV pressure=50.1	Amory et al. (1992)
			Systolic PA pressure=32.2	Amory et al. (1992)
			Systolic RA pressure=5	Reeves et al. (1962)
Pulmonary valve	10	11.9	Diastolic PA pressure=14.5	Amory et al. (1992)
			Diastolic RV pressure=2.6	Amory et al. (1992)

a year (Butcher et al., 2011). During these cardiac cycles, the heart pumps about 3–5 l of blood through the valves each minute (Butcher et al., 2011), which results in a high blood velocity of 1.35 ± 0.35 m/s through the aortic valve (Otto, 2001), and physiological transvalvular pressures of 10 mmHg and 80 mmHg for the pulmonary and aortic valve, respectively (Guyton, 1976).

Please cite this article as: Hasan, A., et al., Biomechanical properties of native and tissue engineered heart valve constructs. Journal of Biomechanics (2013), http://dx.doi.org/10.1016/j.jbiomech.2013.09.023

Table 1 shows the transvalvular pressures for human and bovine valves (Engelmayr et al., 2005). While the accurate *in vivo* shear stress and flexure that the valves experience are still not precisely known, estimated values of 10–80 dyne/cm^2 for shear stress on the aortic valve have been suggested (Weston et al., 1999). Some studies have reported the peak shear stress values to be in the range of 30–1500 dyne/cm^2, where the higher values are correlated to the diseased states, *e.g.* degree of stenosis (Nandy and Tarbell, 1987; Weston et al., 1999). The *in vivo* strain in the circumferential direction for the aortic valve leaflet has been calculated to be 10% and that in the radial direction has been estimated to be 40% (Brewer et al., 1977; Missirlis and Armeniades, 1976; Thubrikar et al., 1980), while that of the aortic root is 5% in both longitudinal and circumferential directions. The cusp extensibility in the radial and circumferential directions are E_r=0.6–0.8 and E_c=0.2–0.3 where E_r and E_c are the Lagrangian strain in the radial and circumferential direction respectively (Lagrangian strain is one of the types of strain).

The minimum (diastolic) pressure occurs toward the beginning of the cardiac cycle when the ventricles are filled with blood while the peak pressure is termed as systolic pressure and it occurs toward the end of the cardiac cycle when the ventricles are contracting. The majority of stresses and strains occur in aortic valve leaflets in the diastolic cycle and during the early opening of valve (Butcher et al., 2011). Assuming that valves get deformed by the blood flow through combined axial stretching and bending, Thubrikar et al. (1980) used elementary beam mechanics theories and calculated the total stresses in the leaflets in systole and diastole to be 50 kPa and 500 kPa, respectively. Other studies estimated the maximum physiological stress of the leaflet to be between 200 and 400 kPa (Christie, 1992; Lee et al., 1984). The elastic modulus in the radial and circumferential directions during initial loading phase have been found to vary in the range of 2–10 kPa and 20–100 kPa respectively, while in the post-non-linear-transition phase it is 1–2 MPa and 8–12 MPa in the radial and circumferential direction respectively. The ultimate tensile strength of the leaflets are 10 folds higher compared to the *in vivo* maximum stresses, and are in the range from 2 to 4 MPa (Leeson-Dietrich et al., 1995). These values can be taken as the guidelines or the targeted ranges for stresses and strains in designing implantable TEHVs, *i.e.* the material to be used in fabrication of a TEHV should have sufficiently high ranges of mechanical properties to function effectively at these ranges of stresses and deformations.

4. Mechanical properties of native and tissue engineered HV constructs

Biomechanical characterizations of human native heart valves are rare in literature due to the limited availability of fresh human heart valves (Clark, 1973; Stradins et al., 2004). Few studies have so far investigated the properties of human heart valves (Balguid et al., 2007; Stradins et al., 2004), while a considerable number of studies have been presented on properties of animal native heart valves such as porcine (Anssari-Benam et al., 2011; Carew et al., 2003; Christie and Barrattboyes, 1995; Gloeckner et al., 1999; Lewinsohn et al., 2011; Merryman et al., 2006; Mirnajafi et al., 2006; Sauren et al., 1983; Stella et al., 2007; Stella and Sacks, 2007) and ovine (Hoerstrup et al., 2000; Sodian et al., 2000a) heart valves. Some studies (Mavrilas and Missirlis, 1991) investigated both human and porcine heart valves. However, each of these studies focused on certain specific mechanical properties. For example, Balguid et al. (2007) tested nine cadaveric aortic valves from healthy individuals (six females and three males, with a mean age of 48.9 ± 11.4 yr), as obtained from deceased patients who had not suffered from aortic heart valve disease. The tissues were stored at 4 °C and were tested at room temperature within 24 h of death. The focus of their investigation was the correlation between biomechanical properties of the heart valve leaflets and collagen-crosslinks. However, the tested mechanical properties included only uniaxial tensile tests.

Stradins et al. (2004) studied 11 healthy cadaveric pulmonary and aortic heart valves from donors between 20 and 50 years old. The valves were maintained in standard physiological solution. They reported only the uniaxial tensile stress–strain behavior too. Another study performed by Mavrilas and Missirlis (1991), reported the mechanical features of human aortic heart valve in which five heart valves, one from female (death due to poisoning) and four from males (death due to traffic accidents) of age 15–27 yr were tested. Similarly, other studies involving biomechanical properties of animal native heart valves and TEHVs mostly focused on investigation of uniaxial tensile mechanical properties. In this review we, therefore, start our discussion with the tensile mechanical properties, which is followed by other mechanical properties including flexural, fatigue and viscoelastic properties.

4.1. Tensile properties

4.1.1. Uniaxial tensile properties

Uniaxial tensile testing is perhaps the most common means of measuring the mechanical properties of heart valves (Grashow et al., 2006b). Fig. 2(a) demonstrates a representative example of stress–strain curve for soft tissues such as heart valve leaflets. In Fig. 2(a), the tensile stress, σ, is defined as, $\sigma=F/A$, where F is the applied force and A is the area of cross section in the released state. The tensile strain, ε, is defined as, $\varepsilon=\Delta L/L_0$, where ΔL is the change in the length of the specimen, and L_0 is its initial length. The elastic modulus, also known as Young's modulus, is defined by the ratio of stress and strain, given as, $E=\sigma/\varepsilon$.

Fig. 2(a) shows that the stress–strain behavior of soft biological tissues such as a heart valve leaflet is highly non-linear. The convention used in description of different mechanical properties of soft tissues from a tensile stress–strain curve is also shown in Fig. 2(a). The parameters E_H, ε_o, and ε_{tr} shown in Fig. 2(a) are called the high elastic modulus, zero-stress extrapolated strain and the transition strain, respectively, and are introduced to facilitate the comparison of the non-linear transition region of different samples (Mavrilas and Missirlis, 1991). The tensile stress–strain curve can be split into a number of regions or phases whose characteristics might be associated with specific physiological functions. The main phases of the curve are (i) low stress–low strain pre transition linear elastic phase, which can be linked to the straightening of the crimped fibers of collagen and the elongation of the elastin fibers, (ii) the highly non-linear transition phase that might be related to the transfer of force from the elastin to the collagen fibers, (iii) a post-transition linear elastic region linked with elongation of elastic and collagen fibers, and (iv) a non-linear region of decreasing stress where the elastin and collagen fibers rupture until complete tearing apart of the tissue.

4.1.1.1. Uniaxial tensile properties of native HV. A number of studies exist in literature on the uniaxial tensile mechanical properties of native aortic and pulmonary heart valves from humans and animal models (Auger et al., 2013). A comparison of the moduli of elasticity of different components of human aortic and pulmonary valves is presented in Table 2 (Stradins et al., 2004). The table shows that except sinuses of valsalva, all elements of aortic valve are more elastic compared to those of pulmonary valve. A collection of stress–strain curves in the circumferential and radial directions for native aortic and pulmonary heart valves is shown in Fig. 2(b) for human, porcine and ovine heart valves.

Please cite this article as: Hasan, A., et al., Biomechanical properties of native and tissue engineered heart valve constructs. Journal of Biomechanics (2013), http://dx.doi.org/10.1016/j.jbiomech.2013.09.023

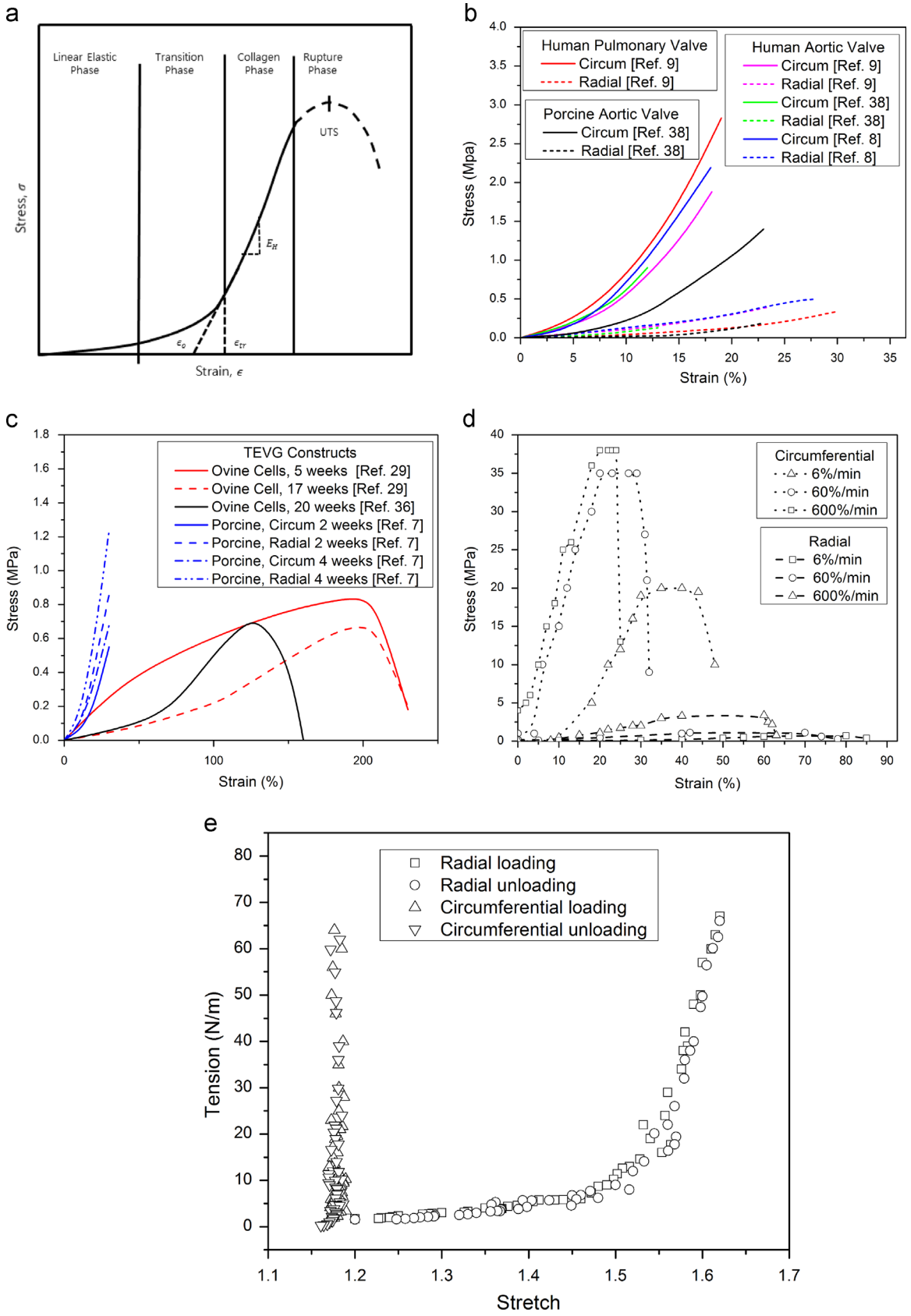

Fig. 2. Uniaxial and biaxial tensile mechanical properties of heart valves: (a) a typical uniaxial tensile stress–strain curve for soft biological tissues such as human aortic and pulmonary heart valve leaflets, (b) uniaxial tensile stress–strain curves for human and animal models native aortic and pulmonary valves in circumferential and radial directions, (c) uniaxial tensile stress–strain curves for TEHV constructs, (d) strain rate sensitivity of uniaxial tensile stress–strain curve for human aortic valve (Mavrilas and Missirlis, 1991). (e) Biaxial loading and unloading tension–stretch data for human aortic valve in the circumferential and radial directions.
Figures reprinted from Sacks et al. (2009) with permission from Elsevier Science.

Please cite this article as: Hasan, A., et al., Biomechanical properties of native and tissue engineered heart valve constructs. Journal of Biomechanics (2013), http://dx.doi.org/10.1016/j.jbiomech.2013.09.023

Table 2
Comparison of moduli of elasticity, E (MPa), of pulmonary and aortic valve elements (Stradins et al., 2004).

	Commissures	Fibrous ring	Sinotubular junction	Sinuses	Reference
Pulmonary valve	10.04 ± 2.82	10.06 ± 2.64	5.85 ± 1.62	14.28 ± 3.48	Stradins et al. (2004)
Aortic valve	13.80 ± 3.16	12.50 ± 2.98	7.41 ± 2.34	10.53 ± 3.22	Stradins et al. (2004)
	$P=0.07$	$P>0.2$	$P>0.2$	$P=0.12$	

Table 3
Uniaxial tensile mechanical properties: Young's modulus, ultimate tensile strength, and strain at maximum stress of tissue engineered and native heart valves (Balguid et al., 2007; Sodian et al., 2000a).

	Young's modulus (MPa)	Ultimate tensile strength (MPa)	Strain[a] $\in_{max}$ (%)	References
Native circumferential	15	2.6	22	Balguid et al. (2007)
Native radial	2	0.4	30	Balguid et al. (2007)
Tissue engineered static	3	0.7	33	Balguid et al. (2007)
Tissue engineered dynamic	6	0.9	25	Balguid et al. (2007)
Unseeded PHO	0.705	0.732	61	Sodian et al. (2000a)
Tissue engineered conduit wall (1 week *in vivo*)	1.325	0.967	10	Sodian et al. (2000a)
Unseeded control of the conduit wall (5 weeks *in vivo*)	1.279	0.955	9	Sodian et al. (2000a)
Tissue engineered conduit wall (5 weeks *in vivo*)	0.487	0.838	88	Sodian et al. (2000a)
Tissue engineered conduit wall (17 weeks *in vivo*)	0.140	0.648	101	Sodian et al. (2000a)
Native pulmonary artery	0.040	0.385	91	Sodian et al. (2000a)

[a] Strain at ultimate tensile stress.

Table 4
Uniaxial tensile mechanical properties, average values of E_H, ε_o, and ε_{tr}, of human and porcine heart valves (mavrials and missirlis).

E_H (MPa)		ε_{tr} (%)		ε_o (%)		References
Circum	**Radial**	**Circum**	**Radial**	**Circum**	**Radial**	
Human aortic valve						
14.55 ± 3.7	1.57 ± 0.18	6.8 ± 1.96	6.9 ± 1.69	3.84 ± 1.40	4.40 ± 1.10	Mavrilas and Missirlis (1991)
7.1	2.27	11	23.9	–	–	Missirlis (1973)
8.33	2.45	–	–	–	–	Armeniades et al. (1973)
5.86	1.70	13	24	–	–	Clark (1973)
13.1	7.50	9	13	–	–	Yamada (1973)
Porcine aortic valve						
7.78 ± 1.7	1.28 ± 0.34	16.8 ± 6.5	11.60 ± 3.10	10.80 ± 5.0	7.50 ± 2.40	Mavrilas and Missirlis (1991)
9.26	2.28	39	51	–	–	Tan and Holt, (1976)
3.35	1.09	33	58	–	–	Chong (1977)
28	1.33	6	12	–	–	Sauren et al. (1983)
6.6	–	8	–	–	–	Rousseau et al. (1983)

Young's modulus, ultimate tensile stress, and maximum strain at failure are shown in Table 3 while the E_H, ε_o, and ε_{tr}, are summarized in Table 4. A large scatter in the literature data is evident for the mechanical properties of native heart valves (Fig. 2b, and Tables 3 and 4). While biological variability accounts for the scatter of the data to some extent, experimental variations are responsible for the rest. The experimental variations arise due to a lack of pre-established standards and inconsistency in specimen preparation, test conditions and measuring parameters such as strain rates, target loads, specimen size and dimensions. Furthermore, inconsistency in the method of extraction of material parameters from highly non-linear material testing data is another reason for the large scattering (Karimi et al. 2008). A comparison of the data from literature therefore require due attention.

It is also evident that the modulus of elasticity and ultimate tensile stress of heart valve leaflets are higher in the circumferential direction than those in the radial direction (Fig. 2(b), Tables 3 and 4). Thus, heart valves are inherently highly anisotropic in nature. Comparison between pulmonary and aortic valves shows that although in a native environment pulmonary and aortic valves experience different transvalvular pressures, the mechanical properties of the two valves are comparable to each other. This justifies the success of clinical practice of substituting aortic valves with the autograft pulmonary valves using the Ross procedure (Chambers et al., 1997; Gerosa et al., 1994; Ross et al., 1992; Stradins et al., 2004).

A significant difference between human valves and those of common animal models such as porcine, bovine, or ovine valves is evident. The animal heart valves are much weaker compared to human heart valves (Fig. 2, Tables 3 and 4). This is one of the reasons that xenograft valve transplants in humans lack long-term durability.

4.1.1.2. Uniaxial tensile properties of tissue-engineered HV constructs. Despite the extensive research on tissue engineering of heart valves over the last few decades, there have been few studies in which complete heart valve constructs have been fabricated. The number of TEHV constructs that advanced to animal studies is even more limited. Studies in which the mechanical properties of the TEHV constructs have been investigated include those of Driessen et al. (2007), Balguid et al. (2007), Engelmayr et al. (2005, 2006), Sodian et al. (2000a) and Hoerstrup et al. (2000) (Fig. 2c).

Driessen et al. (2007) used a biodegradable scaffold of a polyglycolic acid (PGA) mesh with outer coating of polyhydroxybutyrate

Please cite this article as: Hasan, A., et al., Biomechanical properties of native and tissue engineered heart valve constructs. Journal of Biomechanics (2013), http://dx.doi.org/10.1016/j.jbiomech.2013.09.023

(P4HB) to produce a TEHV leaflet. Scaffolds, seeded with cells from human vena saphena magna, were conditioned in a bioreactor with a diastolic pulse duplicator. The leaflets were characterized *in vitro*, and were tested for uniaxial tensile properties along the circumference and radius. The observed properties were then introduced into a computational model to further analyze the mechanics of TEHV.

Balguid et al. (2007) also used non-woven PGA scaffolds coated with a thin P4HB and seeded them with human venous myofibroblast cells to obtain heart valve constructs. Fibrin was used as a cell carrier. One group of the samples were cultured under static environment, while another group, after five days of static culturing, was subjected to dynamic straining for three weeks, at a frequency of 1 Hz. Uniaxial tensile tests were performed on all samples. The results showed that replicating the composition of the extracellular matrix in TEHVs, such as mimicking the collagen content of native heart valve, does not necessarily ensure sufficient mechanical properties. Rather, the nano- and microstructure of the ECM, *e.g.* the density of collagen crosslinks per helix of collagen, seemed to be more important. In addition, the dynamic preconditioning of the constructs resulted in higher elastic modulus and tensile strength compared to static culturing.

The longest implantation study of TEHV so far has been reported by Hoerstrup et al. (2000), Shinoka et al. (1996), and Sodian et al. (2000a). The authors first constructed a single valve leaflet for replacement of pulmonary valve leaflet using PGA mesh scaffold and autologous cells from a sheep. The tissue engineered valve was then implanted into the very same animal (Shinoka et al., 1996). The initial high stiffness of PGA, the poor mechanical properties and the lack of seminal growth of the implanted construct were observed as issues of concern. Hence the authors in their subsequent work adopted polyhydroxyoctanoate (PHO) (Sodian et al., 2000b) scaffolds. They seeded the scaffolds with autologous ovine carotid arterial cells and implanted them into six lambs. Echocardiography data analysis confirmed no stenosis or thrombosis for up to 20 weeks. However, the slow degradation of the PHO, resulting in a prolonged bioabsorption turned out to be of concern. The authors, next, chose PGA mesh coated with a thin layer of P4HB for their scaffold (Hoerstrup et al., 2000). Since P4HB offers higher initial strength and flexibility, due to its thermoelastic nature and shorter biodegradation time, the PGA-P4HB composites offered a good combination of porosity (from PGA) and mechanical properties (from P4HB). The PGA-P4HB autologous tissue engineered valves were reported to function *in vivo* for up to five months and resembled the heart valve structure, mechanics and matrix compositions. The uniaxial tensile stress–strain curve for human aortic valve was highly sensitive to the rate of deformation, *i.e.* the strain rate, in both radial and circumferential directions (Fig. 2(d)), an indication of stress dissipation and relaxation behavior at lower strain rates.

Thus a large number of studies report the uniaxial tensile properties of both native heart valves and TEHV constructs. However, as noted earlier the static uniaxial tensile tests are too simplistic and do not represent the physiological loading conditions on heart valve leaflets *in vivo*. For better characterization, dynamic biaxial and flexural properties of leaflets are more relevant as discussed below.

4.1.2. Biaxial properties

While there are substantial data in literature on the uniaxial tensile mechanical properties of heart valves, data on biaxial tensile mechanical properties (Christie and Barrattboyes, 1995; Grashow et al., 2006b; Martin et al., 2011; Sun et al., 2003), especially time dependent biaxial data, is limited (Stella et al., 2007; Stella and Sacks, 2007). Fig. 2(e) shows biaxial tension–stretch loading–unloading data for a human aortic valve. The leaflet responses in the circumferential and radial directions are clearly distinctive (Fig. 2e). Collagen architecture of aortic and pulmonary valves in its initial state is organized in the circumferential direction of the leaflet. The collagen fibers lay-down pattern defines the response to biaxial tension (Merryman et al., 2006). In the initial stage of the test (small deformation), the collagen fibers are stretched circumferentially and exhibit a rapid rise in tensile stress with a minor increase in strain. The leaflet response in the radial direction takes place in two stages. In the first stage, a toe region exists where a small change in tensile stress causes a large deformation. In the second stage the tensile stress rises steeply until the tissue attains its ultimate extensibility. The toe region in the initial stage can be explained by the fact that the valvular leaflets do not have many aligned fibers along their radial direction. The high compliance of the leaflet along its radial direction in the first stage of the tensile test allows leaflets to be stretched in the diastolic cycle, while the circumferential stiffness is important for supporting the high transvalvular pressure. Such anisotropic properties of the valve leaflets are important for proper valve functioning (Merryman et al., 2006).

The most commonly used biaxial tensile test of the valve leaflets was described in detail in the papers of Grashow et al. (2006a, 2006b), Stella and Sacks (2007). It was recommended that during the tests, specimens should be immersed in PBS solution at physiological temperature. The tensile loads were applied to the specimen through sutures connected along the specimen edges.

The time dependent response of heart valve constructs is of special interest. Stella and colleagues (Stella et al., 2007) studied biaxial time-dependent tensile behavior of porcine aortic valve leaflets. Their study included creep, strain rate and stress relaxation under planar bi-axial stretch from 0 to 60 N/m. The tension *versus* stretch (force–displacement) relation was found to be insensitive to the strain rate. While a low level of hysteresis (17%) and a significantly high level of stress-relaxation (~27.5% in circumferential direction, 33.3% in radial direction) were observed, the exhibited creep was negligible over 3 h. These results contradict the earlier findings on ligaments and pericardium, all of which exhibited significant creep. This indicates that the relaxation and creep mechanisms in the heart valves are not dependent on each other.

Sacks et al. (2009) developed a series of tests that enabled micro-structural insights into the mentioned phenomenon. By applying small angle X-ray scattering (SAXS) the authors probed the dependence of mechanical properties of the tissues on the kinematics of collagen fibrils under biaxial stress. In creep tests carried out for 60 min, both the tissue strain and fibril D-period strain remained constant. In case of stress relaxation the fibril D-period strain decreased rapidly in the first 10 min of the 90 min test. The authors concluded that the stress relaxation can be due to an internal slipping mechanism, probably regulated by non-collagenous components, such as proteoglycans, whereas the lack of creep in presence of stress relaxation suggested that no internal slipping was present under constant loads (only under constant external strains). However, the study was performed on mitral valve leaflets as opposed to aortic or pulmonary valve. Investigations on time dependent biaxial properties of aortic and pulmonary valve might reveal similar or more useful insights.

4.2. Flexural/bending properties

Flexure/bending (Figs. 3(a)–(c)) is a major deformation mode for heart valve leaflets. Although uni-axial and biaxial tensile experiments - conducted on excised strips of valve leaflets - dominate documented studies (Anssari-Benam et al., 2011; Sacks et al., 2009; Sacks and Yoganathan, 2007; Stella et al., 2010; Vesely,

Please cite this article as: Hasan, A., et al., Biomechanical properties of native and tissue engineered heart valve constructs. Journal of Biomechanics (2013), http://dx.doi.org/10.1016/j.jbiomech.2013.09.023

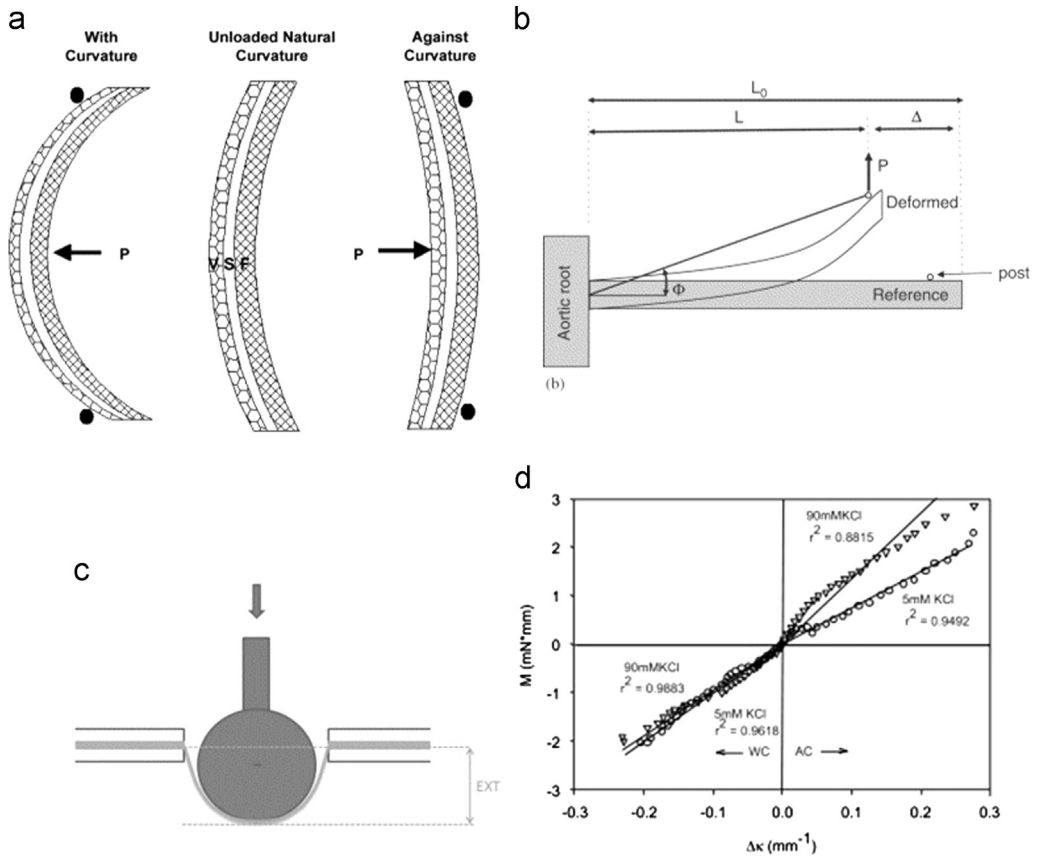

Fig. 3. The different testing methods for flexural properties of aortic heart valve tissue, (a) three-point bending (Merryman et al., 2006a): the tissue is supported on two beams and indented by a third beam, (b) cantilever bending (Mirnajafi et al., 2006): the valve tissue remains connected to the aortic root (fixed side) and a post is attached to the free side which induces cantilever bending, (c) flexural macro-indentation test (Ragaert et al., 2012): The leaflet is clamped over a round opening and indented with a ball probe, (d) Flexural mechanical properties: *M versus* $\Delta\kappa$ relations (Sacks et al., 2009).
Figures reprinted with permission from Elsevier Science.

1998; Vesely and Noseworthy, 1992; Wang et al., 2005; Weinberg et al., 2010), these tests do not fully represent the physiological deformation of the valves. The actual physiological deformation of heart valves is largely a flexural deformation. An added advantage of using flexural tests is the fact that they allow for the quantification of strains at comparatively low stresses.

Flexural tests were first conducted on heart valve leaflets in the late 1980s (Vesely and Boughner, 1989) when the calcification of glutaraldehyde-fixed porcine prosthetic valves was attributed to flexural stresses (Sabbah et al., 1985, 1986), turning the bending properties of leaflets into a clinically relevant topic. The first flexural experiment (Vesely and Boughner, 1989) employed a modified form of the three-point bending test method, in which the leaflet strips were positioned vertically between two clamps that preloaded the tissue to a flattened state. By rotating the top clamp by 90° the tissue strip was bent over a mandrel. The bending moment and flexural stiffness of the tissue were then calculated using simple beam theory. The authors observed that the bending stiffness, S_n, increased with the (tensile) stress applied by the upper clamp according to the second-order polynomial relation Eq. (1), given by

$$S_n = 100 + 2.1\sigma + 0.083\sigma^2 \quad (1)$$

where S_n is the bending stiffness, in nN m² unit, and σ is the applied stress in kPa. They also reported that the bending stiffness was only slightly affected by the preload applied to the tissue. Furthermore, it was observed that the neutral fibers of the deformed tissue were not located in the central plane of the cross section, but closer to the side of the fibrosa. Since a centrally located neutral plane is a prerequisite for the application of simple beam theory, the authors suggested that this theory did not apply to their experimental setup.

The flexural test experiments performed on heart valve leaflets can largely be classified into three categories: three-point bending tests, cantilever bending tests and macro-indentation tests. Cantilever and three-point bending are typically conducted on excised strips of tissue, while macro-indentation tests are performed on the entire valve leaflet. A schematic overview of these three flexural test methods is shown in Figs. 3(a)–(c), and brief descriptions of these different tests are provided below. Unless indicated otherwise, all research summarized in this section were conducted on porcine aortic valve tissues and on samples extracted from the belly region, the central tissue region, of the leaflets.

4.2.1. *Three-point bending*

A considerable volume of work on three-point bending properties of aortic valve leaflets has been reported by Sacks et al. One example is the work conducted by Gloeckner et al. (1999), in which the authors investigated the effects of fatigue on aortic valve bending properties. The bending stiffness, *EI*, was obtained using the linear beam theory, according to the formula

$$EI = \frac{FL^3}{48y_{max}} \quad (2)$$

where F is the applied force, L is the span length between the two supports, and y_{max} is the maximum depth of indentation. The authors reported the experimental results in terms of a bending stiffness index (BSI), meant to serve as a basis for comparison of

bending stiffness among samples. A mean BSI of 4.0×10^4 N m² was obtained in the circumferential direction, while a four times lower mean BSI was obtained in the radial direction, both for bending along the physiological direction of curvature. The BSI value almost doubled for bending against curvature in the circumferential direction, while no significant difference was noticed in the radial direction. In terms of fatigue, the decrease of the BSI for up to 200 million loading cycles was quantified. The results will be discussed in the fatigue properties section. The observed differences in the non-fatigued BSI value were attributed to the complex structure of the valve tissue: the preferential orientation of the collagen fibers along the circumferential direction was responsible for the higher BSI in this direction. Also, when bending the leaflet against the natural curvature direction, the fibrosa was stretched and the ventricularis was compressed (opposed to the bending in the curvature direction in which fibrosa is compressed and ventricularis is stretched). Being thicker and composed primarily of dense collagen fibers, the fibrosa contributes the most to circumferential bending properties and thus increases bending stiffness in the adverse direction.

Based on Gloeckner's method, Engelmayr et al. (2003) developed a bioreactor specifically designed to subject TEHV to cyclic (uni-directional or two-way) flexure and included an evaluation of scaffold bending stiffness for dynamic culture periods of up to five weeks. For determining the effective stiffness of the tissue constructs, they introduced a method based on visual monitoring of markers which represented the deformation of the samples. From these, they calculated the applied moment M and the change in curvature $\Delta\kappa$, which were plotted against each other. Through regression, a linear relationship was determined between the two and finally the effective stiffness was obtained from the slope of this linear curve (Fig. 3(d)) using the Bernoulli–Euler moment–curvature relationship (Frisch-Fay, 1962)

$$M = E_{eff} I \Delta\kappa \tag{3}$$

In Eq. (3), the slope $E_{eff}I$ is the flexural rigidity of the sample, with E_{eff} being the effective stiffness and I the second moment of inertia. Dividing this slope by I yields the effective stiffness value of the sample. By using the change in curvature, the authors effectively worked around the problem that the tissue was not taut over the supporting beams in a conventional three-point bending setup (Vesely and Boughner, 1989), as can also be observed in Fig. 3(a).

The incubation of (unseeded) non-woven polymeric mesh scaffolds under dynamic flexure conditions led to a substantial decrease in effective stiffness for these scaffolds, while the loss of stiffness was significantly less severe for statically cultured scaffolds. In a follow-up study (Engelmayr et al., 2005), the scaffolds were seeded with ovine smooth muscle cells (SMC), which led to increased stiffness after three weeks of culture, as the cellular component could contribute to the overall scaffold stiffness. It could also be shown that the flexing of the scaffolds during incubation led to a 63% increase in developed collagen compared to the static group.

Using the same three-point bending method, Merryman et al. (2006) investigated the effect of aortic valve interstitial cell (AVIC) contraction on the flexural stiffness. They performed the bending test on valve leaflets after eliciting a cellular contraction, and after inhibiting cellular contraction. Effective stiffness values of 150–200 kPa were reported, with an overall independence of stiffness from bending direction and flexural angle. It was also found that the mechanical contribution of the AVIC to the bending stiffness was largely negligible.

Furthermore, the three-point bending test method first developed by Gloeckner has been used for the evaluation of porcine heart valve prosthetics (Mirnajafi et al., 2006) as well as pericardial porcine heterografts for valve leaflets (Mirnajafi et al., 2005). However, these results are considered beyond the scope of this review.

4.2.2. Cantilever bending

Cantilever bending is physiologically relevant to the local deformation near the commissural region of the leaflet, which - contrary to the belly region - is connected to the aortic root and is in contact with other leaflets. Its attachment to the aortic root may be abstracted to the fixed end of a simple beam under cantilever bending. Mirnajafi et al. (2006) adapted Gloeckner's device (Gloeckner et al., 1999) to cantilever bending test as shown in Fig. 3(b). Once again based on simple beam theory, the effective stiffness was determined as a function of the flexural angle ϕ, for angles between 22° and 40°. A linear $E-\phi$ relation was established for bending both along and against the physiological direction. For the sake of comparison, an instantaneous E_{eff} was chosen at $\phi = 30°$, This E_{eff} was found to be about one third of the value for the belly region, previously determined by Merryman et al. (2006), when bending along the physiological direction. Contrary to earlier results for bending of the belly region, the stiffness in the commissural region was found to be significantly sensitive to the direction of the bending: it was roughly 50% stiffer when bent against the physiological direction.

4.2.3. Macro-indentation

In flexural macro-indentation tests, the excised valve tissue is clamped over a round opening and indented with a ball probe, resulting in a load *versus* depth of indentation curve. The major difference with respect to three-point bending tests is that the flexural response of the entire leaflet is tested, as opposed to cut-out strips, whose behavior is dependent on the direction in which they are cut. Although the entire valve leaflets are used, it is the flexural behavior of the belly region that is evaluated, as the commissural region remains inside the clamped part.

The macro-indentation tests of aortic valve tissue were first reported by Narine et al. (2006), who investigated the effects of cryopreservation on decellularized porcine valves meant for prosthetic use. The authors reported that while cryopreservation did not significantly affect the maximum stress at failure of the leaflet, it did increase the strain at failure. The authors recalculated the obtained load indentation curves to determine stress–strain equivalents. From the depth of indentation, the contact surface area between ball probe and leaflet were calculated geometrically, which was used to convert the measured load to stress. Likewise, the strain was obtained by comparing the contact surface area to the circular opening in the plate. Using this method, the principles of uni-axial tensile straining was applied to a case of flexural loading. As such, these results should be interpreted with care. Narine et al. (2006) investigated only the ultimate properties of the valve leaflets, reporting on stress and strain at break. While these may yield useful information, they reveal little of the functional behavior of the valve, more specifically an indication of flexural stiffness in the lower stress regions.

A new series of experiments was recently conducted by Ragaert et al. (2012). A schematic for their test method is shown in Fig. 3(c). In order to consider the strain hardening of the tissue by previous loading, the leaflets were preloaded twice before the relevant tissue properties were determined. The properties include: the *maximum load* – the maximum applicable load on the cusp (ML) [N], *extension at break* – indentation depth prior to rupture (EXT) [mm], and the *stiffness parameter* – the linear slope of the load–indentation curve (ST) [N/mm] which is a measure of the tissue stiffness. ML and EXT present the characteristics of the cusps, while ST gives information about the physiological properties of the tissue. Although not a

Please cite this article as: Hasan, A., et al., Biomechanical properties of native and tissue engineered heart valve constructs. Journal of Biomechanics (2013), http://dx.doi.org/10.1016/j.jbiomech.2013.09.023

value for E_{eff} [N/mm²] as was calculated from the three-point bending tests described above, ST [N/mm] is nonetheless a functional parameter describing the tissue's flexural response to an applied load. The reported values (mean ± st. dev.) for these properties were $EXT = 3.07 \pm 0.68$ mm, $ML = 15.08 \pm 4.29$ N and $ST = 8.97 \pm 1.17$ N/mm. In the experiments, it was also found that the coronary position of the leaflet is irrelevant to their flexural properties. Recently, nano-indentation-based methods have been applied for characterization of various advanced materials, such as metal foams (Kim et al., 2005). These methods also have strong potential in the study of heart valve biomechanics.

Thus the different types of flexural tests including the three point bending, cantilever bending and macro-indentation tests provide complementary insights about the performance of TEHV constructs, and a combination of these tests would be more useful in understanding the flexural performance of the TEHV constructs compared to a single test.

4.3. Viscoelastic properties of heart valves

There have been very few investigations on the viscoelastic properties of the heart valves. Although rheological studies are widely used in a range of scientific and engineering fields, the tissue engineering literature has made little use of rheological or viscoelastic properties. As mentioned above, the viscoelastic properties of leaflets significantly differ depending on the leaflet direction similar to tensile and flexural properties. The mechanical properties of the valve leaflet are strongly anisotropic due to the fact that their fibers are aligned. All valve leaflets are stiffer in the circumferential direction in comparison to the radial direction (Weinberg and Mofrad, 2005).

As valve leaflets are made of viscoelastic material, their stress–strain characteristics are strain rate dependent. Also, even though the stress relaxation and creep phenomena are present, the creep is not significant, Fig. 4(a) and (b) (Stella et al., 2007). Hysteresis is

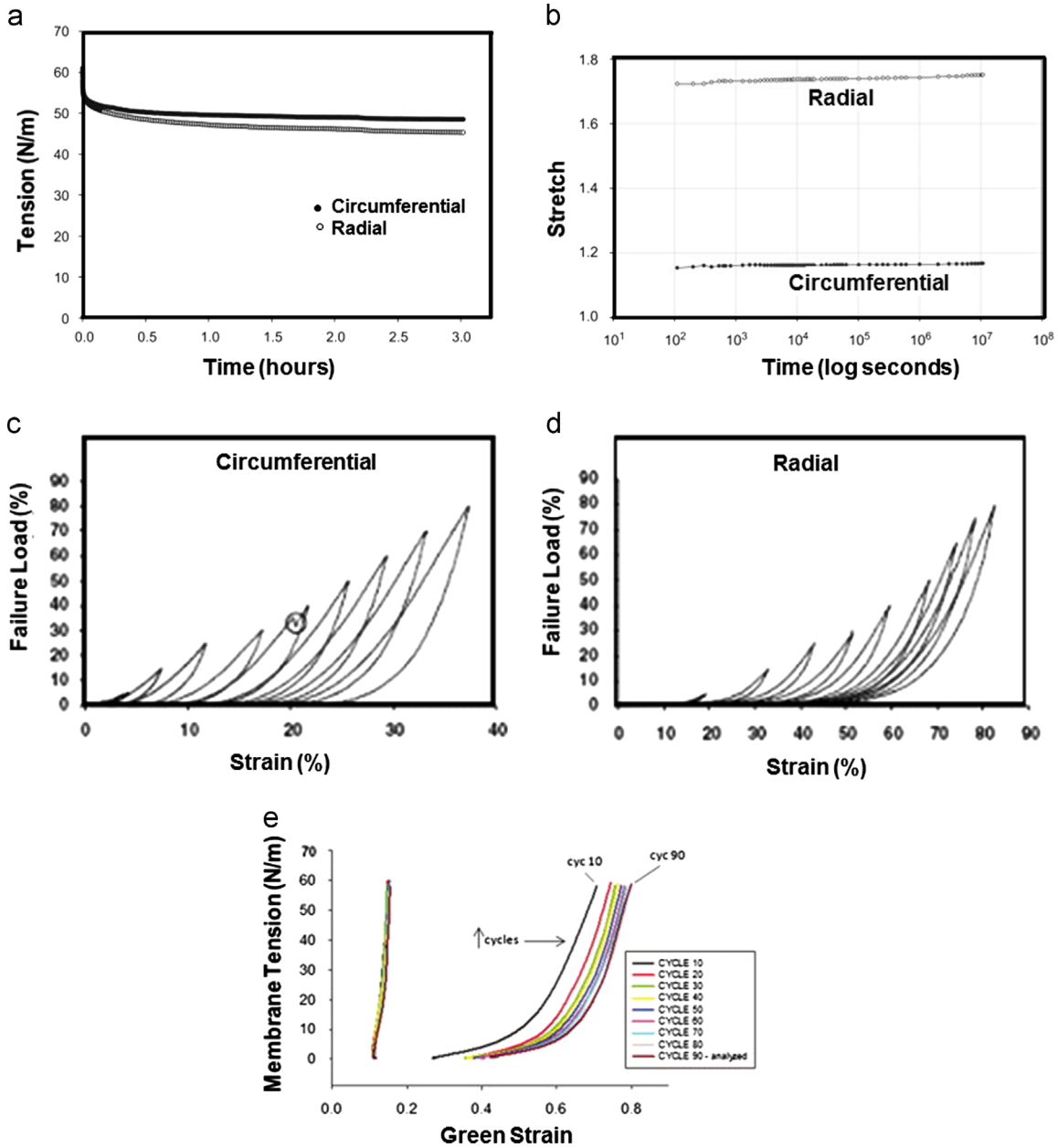

Fig. 4. Illustration of the viscoelastic response of a valve leaflet: (a) relaxation and (b) creep experiment (Stella et al., 2007), (c, d) hysteresis and recoverability of the aortic valve tissue (Anssari-Benam et al., 2011), (e) illustration of the effects of preconditioning of porcine aortic valve on stress–strain characteristic (Martin and Sun, 2012). Figures adapted and reprinted with permission from Elsevier Science.

Please cite this article as: Hasan, A., et al., Biomechanical properties of native and tissue engineered heart valve constructs. Journal of Biomechanics (2013), http://dx.doi.org/10.1016/j.jbiomech.2013.09.023

observed during the cyclic loading, but recoverability is limited to given number of cycles.

A multitude of constitutive models have been proposed for the heart valve tissue. Most of them describe the strain rate and time dependence of the valve material, like the Kelvin–Voigt (Anssari-Benam et al., 2011) model of viscoelasticity, however the most popular approach is to use the quasilinear viscoelastic model (QLV) proposed by Fung (1972). The QLV is the most widely used approach in biomechanics of soft tissues and is useful in describing the viscoelastic behavior of biological materials such as ligament, tendon, cartilage and skin. In the QLV model the stress is represented by Eqs. (4) and (5), separating elastic response and relaxation function (Xu and Lu, 2011) as follows:

$$\sigma(t) = \int_0^t G(t-\tau,\varepsilon)\dot{\varepsilon}(\tau)\,d\tau \tag{4}$$

$$\varepsilon(t) = \int_0^t J(t-\tau,\sigma)\dot{\sigma}(\tau)\,d\tau \tag{5}$$

where τ is a dummy variable and t is the time; σ is the stress, ε is the strain, G is the creep modulus function and J is the relaxation modulus function. In case of quasilinear tissue response, the functions G and J can again be divided into two parts, one that depends on strain and the other that depends on time given by

$$G(t) = g(t)\sigma_e(\varepsilon) \tag{6}$$

$$J(t,\sigma) = j(t)\varepsilon_e(\sigma) \tag{7}$$

where g and j are functions of creep and relaxation. The parameter σ represents the response shown instantaneously, whereas ξ is the elastic strain response.

It was shown that preconditioning of the specimen at a sufficiently large number of loading and unloading cycles results in significant decrease of strain rate dependence, such that the viscous effect disappears, but the material remains non-linearly elastic. The behavior of such preconditioned material could be appropriately described using the hyper elastic model (Figs. 4 (c) and (d)) (Martin et al., 2011).

The hyper elastic material model is based on the fact that the energy density function W depends on the strain state. Stress σ can be obtained from (Martin and Sun, 2012)

$$\sigma = \frac{\partial W}{\partial \varepsilon} \tag{8}$$

One of the most popular energy density functions used for capturing the non-linear behavior of soft tissues is the Fung-type strain energy density function (Martin and Sun, 2012; Weinberg and Mofrad, 2005) expressed by

$$W = \frac{C}{2}(e^Q - 1) \tag{9}$$

where c is fixed and Q is a function of the strain state, given by

$$Q = A_1E_{11}^2 + A_2E_{22}^2 + 2A_3E_{11}E_{22} + A_4E_{12}^2 + 2A_5E_{11}E_{12} + 2A_6E_{22}E_{12} \tag{10}$$

where c and A_i are the material parameters, whereas E_{xy} are the terms of Green strain. Thus it is evident that aside from some mathematical modeling, experimental investigations of the viscoelastic properties have remained largely un-addressed. The in-depth understanding of the viscoelastic properties particularly the stress relaxation, hysteresis *etc.* can help in designing more durable TEHV constructs, as well as in gaining useful insights into pathology of stenosis, calcification and other valvular diseases.

4.4. Fatigue properties

Mechanical fatigue plays an important role in valvular mechanics, both in healthy and pathological conditions. The continuous repetitive cyclic stress from the complex combination of stretching, flexure and shear may cause delamination of the layered leaflet structure through flexion, which may then lead to calcification and further delamination, and finally failure of the valve leaflets (Gloeckner et al., 1999). Accelerated durability tests can be used to induce fatigue in various loading modes on native valves and TEHV constructs to understand their effects on the structure and on long term mechanical properties. However, hardly any data can be found in literature on the fatigue behavior of heart valves except that of Gloeckner et al. (1999) where the authors investigated the effects of mechanical fatigue on the three point bending properties of porcine bioprosthetic heart valves. The valves were fatigued to 0, 50, 100 and 200 million cycles of flexural stress with and against the curvature direction of the valve leaflets. Linear beam theory was also applied. The result, as shown in Fig. 5, revealed that as the number of cycles increased, the bending stiffness of valve leaflets decreased significantly, both in the radial and circumferential directions. The decrease of bending stiffness index against the curvature direction was largest, namely 80% lower after 200 million cycles compared to a valve that had not been exposed to flexural stress.

As the valve leaflets *in vivo* experience about 30 million loading–unloading cycles per year, it is expected that the bending stiffness and other mechanical properties of TEHV constructs would deteriorate over time after implantation. This change in mechanical properties must be taken into account in designing implantable TEHV constructs. However, the quantitative effect of

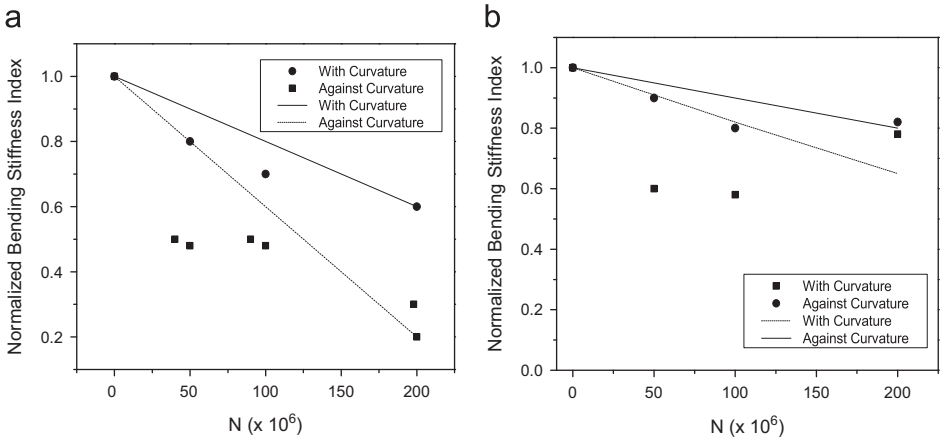

Fig. 5. Effect of fatigue on bending stiffness of heart valves.
Adapted from Gloeckner et al. (1999) with permission from Elsevier Science.

fatigue on the uniaxial and biaxial tensile, flexural and viscoelastic properties of valve leaflets have remained largely unknown. It is imperative that future studies should pay due attention to the *in vitro* characterization of the effect of fatigue on important mechanical properties of TEHV constructs prior to investigation of *in vivo* performance in animals. This can significantly reduce the costs and increase the chance of success in achieving the goal of an implantable TEHV construct.

5. Computational models of heart valve mechanics

Computational models have been developed to aid in understanding the mechanics of healthy and diseased heart valves. While much work has been devoted to developing constitutive equations to describe the mechanics of heart valve tissues (Holzapfel et al., 2000; Weinberg and Kaazempur-Mofrad, 2006; Weinberg and Mofrad, 2005), some groups have developed functional models of heart valves as well (Sun and Sacks, 2005; Weiler et al., 2011; Weinberg and Kaazempur Mofrad, 2007a). Given the multiscale nature of valve biomechanics, linking the scales of cells, tissues and organs, and ultimately to molecular scales, full understanding of the disease mechanisms and processes would necessitate multiscale models that can seamlessly span and link these disparate scales (Weinberg and Kaazempur Mofrad, 2007b). As a first step in this direction, researchers have developed multiscale models for calcification driven aortic stenosis of both the tricuspid and bicuspid valves (Weinberg and Kaazempur Mofrad, 2008). Aortic valve consists of three cusps and surrounding tissues; however some patients have aortic valves with two cusps or leaflets since birth. The bicuspid valves suffer from the calcific aortic stenosis (CAS) more often than tricuspid valves. Normally, in healthy valves, the cusps are thin and pliable. In CAS, calcified nodes may spread all over the cusps. Currently it is not known whether the increase in the risk of CAS is due to the difference in geometries of the valves, or is due to the factors that produce the geometric differences. Weinberg et al. implemented multiscale models of aortic valve and isolated the effect of individual parameters on the mechanics of valves at different scales (Weinberg and Kaazempur Mofrad, 2008). Additionally, the bicuspid and tricuspid valves were modeled considering the scales at the organ, tissue and cell level. Their models were dynamic, 3-D, and considered detailed constitutive behavior. The simulations showed the expected organ level difference between the bicuspid and tricuspid valves. Also, the bicuspid valve demonstrated higher flexure in the solid phase and stronger jet formation in the fluid phase compared to the tricuspid data. From these data it can be inferred that the higher rate of calcification in bicuspid valves compared to tricuspid valves are not merely due to the geometric differences (Weinberg and Kaazempur Mofrad, 2008). A combination of computational and experimental studies will be ideal to further understand the mechanotransduction mechanisms of valvular diseases, such as calcific aortic stenosis (Kaazempur-Mofrad et al. 2005). A recent study (Weinberg et al., 2010) reported that the phenotypes induced *in vitro* to the valvular endothelial cells exposed to the hemodynamic microenvironment of the two sides of the aortic valve are distinct from each other. Understanding the effect of local hemodynamics on the valvular pathogenesis is of high research interest. Researchers have designed specific hemodynamic environment for valve surfaces to perform more illustrative studies. Different waveforms of shear stress, mimicking those from the *in vivo* stresses on the ventricular and aortic sides have been extracted from computational models and applied to the *in vitro* cultured human endothelial cells. Cells experiencing shear waves of the ventricle side exhibited an anti-inflammatory endothelial cell phenotype as opposed to the aortic counterpart. This result shows that computational modeling can be helpful in understanding the mechanotransduction of heart valves in both healthy and pathogenic states. In addition, simulation results from these models can also help in achieving optimum design of TEHV constructs through iterative studies of structure to mechanical properties relationship for different materials.

6. Summary and future directions

A detailed understanding of both the quasi-static and dynamic mechanical properties and the structure–mechanical response relationships of human and animal heart valves is essential to enable the generation of TEHVs and to treat diseased heart valves. However, the inadequacy of data on biomechanical properties of heart valves in the literature is evident. The lack of proper mechanical properties data is still an obstacle for achieving successful design and fabrication of implantable fully functional tissue engineered heart valves with long term durability. Particularly, there has been little work performed on the dynamic biomechanical properties such as fatigue, flexural, and viscoelastic properties of heart valves. The need for more extensive investigations of the biomechanical properties of heart valves is thus inevitable. While the unavailability of fresh human heart valves is an obstacle in obtaining extensive biomechanical data of heart valves, a combined experimental/computational modeling approach can provide extensive insights into structure–biomechanical response relationships from a small number of heart valve samples. Specifically, extensive parametric studies using computational models that have been validated against simple experimental test data will be helpful in design and development of functional TEHV constructs. Defining the most relevant biomechanial properties crucial for the success of functional and implantable TEHV constructs, as well as straightforward experiments in which these properties can be determined are important factors that deserve more attention in future work. Similarly, the appropriate ranges of the scaffold and tissue construct properties required for acceptable functionality limits are also among important factors deserving attention.

Once the critical design criteria and required ranges for various static and dynamic mechanical properties of heart valves are established, designing suitable biomaterials and tissue engineering methods for achieving the desired ranges of properties will be necessary. An overview of common approaches used for tissue engineering of heart valves is depicted in Fig. 6 (modified from Loftin et al., 2011). In brief, scaffolds prepared from various natural or synthetic biomaterials are seeded with various cell types such as endothelial progenitor cells (EPCs), vascular endothelial cells (VECs), smooth muscle cells (SMCs), messenchymal stem cells (MSCs), adipose-derived stem cells, amniotic fluid-derived stem cells *etc.* The cell-seeded constructs can be conditioned *in vitro* using various growth factors, signaling molecules, and/or mechanical stimulations such as shear flow and strain (in suitable bioreactors) for tissue formation and improvement of mechanical and hemodynamic properties. The tissue engineered constructs after preconditioning are implanted in animal models and evaluated for *in vivo* structural, mechanical and biological performances including thrombo-resistance, *in situ* tissue remodeling, integration of the construct with the native tissues, deterioration of mechanical properties with time *etc.* After optimization of the constructs in animal models, the next logical step will be to conduct clinical trials of the constructs in human subjects. Ensuring sufficient mechanical properties in the TEHV will be important prior to clinical trials, and in order to do so, future research in this field should focus not only on designing new biomaterials with improved mechanical

Please cite this article as: Hasan, A., et al., Biomechanical properties of native and tissue engineered heart valve constructs. Journal of Biomechanics (2013), http://dx.doi.org/10.1016/j.jbiomech.2013.09.023

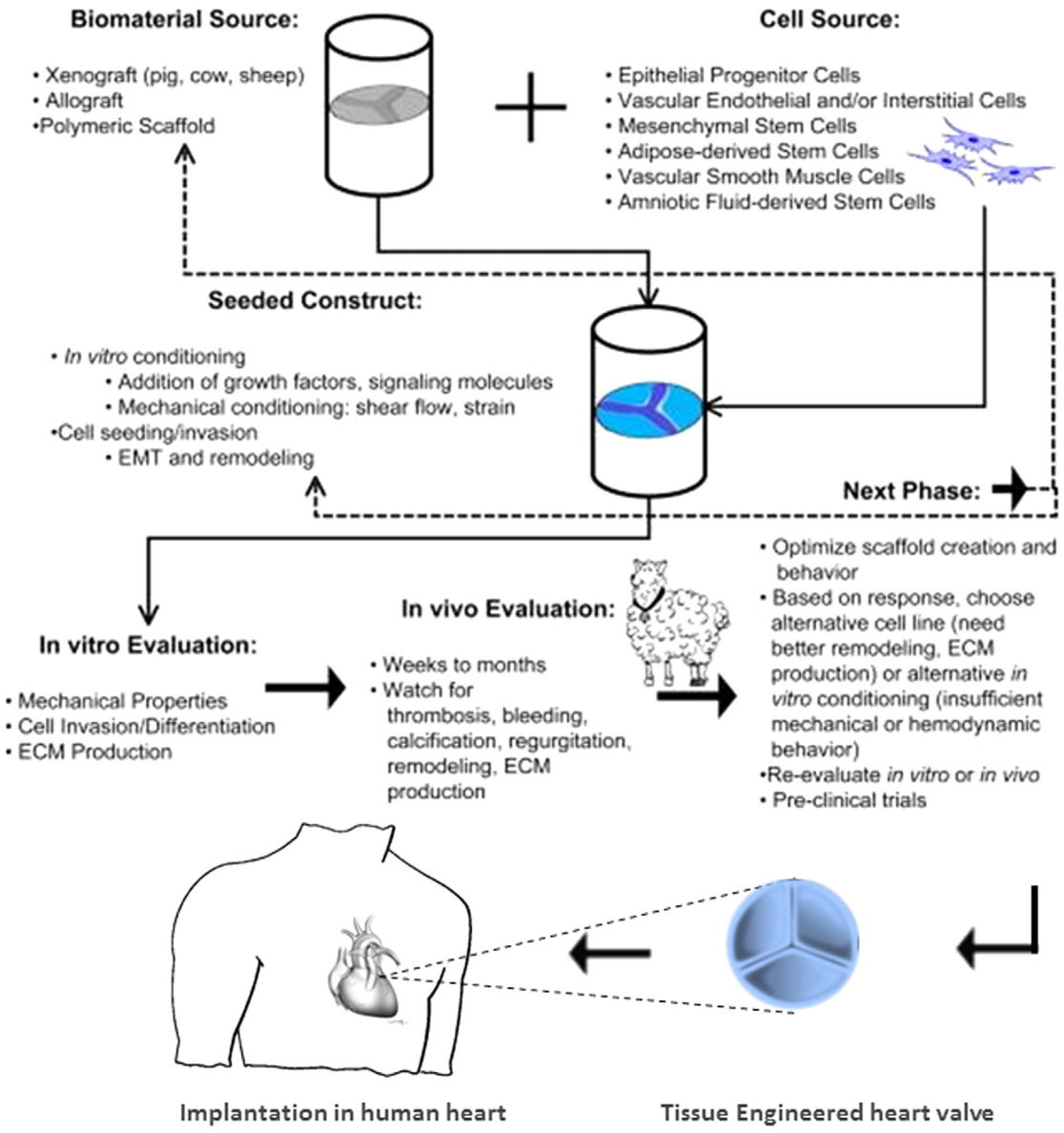

Fig. 6. Common approaches for tissue engineering of heart valves. Scaffolds prepared from various natural or synthetic biomaterials are seeded with desired cell types. The cell seeded constructs are conditioned *in vitro* using various chemical and mechanical cues for tissue formation and improvement of mechanical and hemodynamic properties. The preconditioned engineered tissue constructs are evaluated in animal models. After optimization of the constructs in animal models, the intended step is to implant the constructs in human subjects.
Figure modified and reprinted from Loftin et al. (2011), with permission from Springer Science.

properties but also on designing improved bioreactors for better preconditioning of the TEHV constructs.

Conflict of interest statement

The authors declare that they have no conflict of interest, financial or otherwise, related to the materials discussed in this manuscript.

Acknowledgments

A.H. acknowledges Natural Sciences and Engineering Research Council of Canada (NSERC) postdoctoral fellowship. A.P. acknowledges postdoctoral award from Fonds Québécois de la Recherche sur la Nature et les Technologies (FRQS, Canada). A.K. acknowledges funding from the National Science Foundation CAREER Award (DMR 0847287), the Office of Naval Research Young National Investigator Award, the National Institutes of Health (HL092836, DE019024, EB012597, AR057837, DE021468, HL099073, EB008392), and the Presidential Early Career Award for Scientists and Engineers (PECASE). Authors also acknowledge the help of Arash Nasajpour, a summer student in Ali Khademhosseini lab in organizing some of the data in Tables.

References

Adham, M., Gournier, J.P., Favre, J.P., De La Roche, E., Ducerf, C., Baulieux, J., Barral, X., Pouyet, M., 1996. Mechanical characteristics of fresh and frozen human descending thoracic aorta. J. Surg. Res. 64, 32–34.

Aldous, I.G., Veres, S.P., Jahangir, A., Michael, L.J., 2009. Differences in collagen cross-linking between the four valves of the bovine heart: a possible role in adaptation to mechanical fatigue. Am. J. Physiol. Heart Circ. Physiol. 296, 1898–1906.

Amory, H., Linden, A.S., Desmecht, D.J.M., Rollin, F.A., McEntee, K., Lekeux, P.M., 1992. Technical and methodological requirements for reliable haemodynamic measurements in the unsedated calf. Vet. Res. Commun. 16, 391–401.

Anssari-Benam, A., Bader, D.L., Screen, H.R.C., 2011. A combined experimental and modelling approach to aortic valve viscoelasticity in tensile deformation. J. Mater. Sci.: Mater. Med. 22, 253–262.
Armeniades, C.D., Lake, L.W., Missirlis, Y.F., Kennedy, J.H., 1973. Histologic Origin of Aortic Tissue Mechanics, The Role of Collageneous and Elastic Structures. Wiley, New York.
Auger, F.A., Gibot, L., Lacroix, D., 2013. The pivotal role of vascularization in tissue engineering. Annu. Rev. Biomed. Eng. 15, 177–200.
Balguid, A., Rubbens, M.P., Mol, A., Bank, R.A., Bogers, A., Van Kats, J.P., De Mol, B., Baaijens, F.P.T., Bouten, C.V.C., 2007. The role of collagen cross-links in biomechanical behavior of human aortic heart valve leaflets – relevance for tissue engineering. Tissue Eng. 13, 1501–1511.
Brand, N.J., Roy, A., Hoare, G., Chester, A., Yacoub, M.H., 2006. Cultured interstitial cells from human heart valves express both specific skeletal muscle and non-muscle markers. Int. J. Biochem. Cell Biol. 38, 30–42.
Brewer, R.J., Mentzer Jr., R.M., Deck, J.D., 1977. An in vivo study of the dimensional changes of the aortic valve leaflets during the cardiac cycle. J. Thorac. Cardiovasc. Surg. 74, 645–650.
Butcher, J.T., Mahler, G.J., Hockaday, L.A., 2011. Aortic valve disease and treatment: the need for naturally engineered solutions. Adv. Drug Deliv. Rev. 63, 242–268.
Carew, E.O., Patel, J., Garg, A., Houghtaling, P., Blackstone, E., Vesely, I., 2003. Effect of specimen size and aspect ratio on the tensile properties of porcine aortic valve tissues. Ann. Biomed. Eng. 31, 526–535.
Chambers, J.C., Somerville, J., Stone, S., Ross, D.N., 1997. Pulmonary autograft procedure for aortic valve disease: long-term results of the pioneer series. Circulation 96, 2206–2214.
Chong, M., 1977. Mehanical Studies on the Porcine Aortc Valve Part I (Ph.D. thesis). McMaster University, Hamilton, Ontario.
Christie, G.W., 1992. Anatomy of aortic heart valve leaflets: the influence of glutaraldehyde fixation on function. Eur. J. Cardio-Thorac. Surg. 6, S25–S33.
Christie, G.W., Barrattboyes, B.G., 1995. Mechanical-properties of porcine pulmonary valve leaflets – how do they differ from aortic leaflets. Ann. Thorac. Surg. 60, S195–S199.
Clark, R.E., 1973. Stress–strain characteristics of fresh and frozen human aortic and mitral leaflets and chordae tendineae – implications for clinical use. J. Thorac. Cardiovasc. Surg. 66, 202–208.
Cox, M.A.J., 2009. Local Mechanical Properties of Tissue Engineered Heart Valves. Technische Universiteit Eindhoven/Eindhoven University of Technology.
Doyle, J.T., Patterson, J.L., Warren, J.V., Detweiler, D.K., 1960. Observations on the circulation of domestic cattle. Circ. Res. 8, 4–15.
Driessen, N.J.B., Mol, A., Bouten, C.V.C., Baaijens, F.P.T., 2007. Modeling the mechanics of tissue-engineered human heart valve leaflets. J. Biomech. 40, 325–334.
Du, Y., Lo, E., Ali, S., Khademhosseini, A., 2008. Directed assembly of cell-laden microgels for fabrication of 3D tissue constructs. Proc. Natl. Acad. Sci. 105, 9522–9527.
Durst, C.A., Cuchiara, M.P., Mansfield, E.G., West, J.L., Grande-Allen, K.J., 2011. Flexural characterization of cell encapsulated PEGDA hydrogels with applications for tissue engineered heart valves. Acta Biomater. 7, 2467–2476.
Engelmayr, G.C., Hildebrand, D.K., Sutherland, F.W.H., Mayer, J.E., Sacks, M.S., 2003. A novel bioreactor for the dynamic flexural stimulation of tissue engineered heart valve biomaterials. Biomaterials 24, 2523–2532.
Engelmayr, G.C., Rabkin, E., Sutherland, F.W.H., Schoen, F.J., Mayer, J.E., Sacks, M.S., 2005. The independent role of cyclic flexure in the early *in vitro* development of an engineered heart valve tissue. Biomaterials 26, 175–187.
Engelmayr, G.C., Sales, V.L., Mayer, J.E., Sacks, M.S., 2006. Cyclic flexure and laminar flow synergistically accelerate mesenchymal stem cell-mediated engineered tissue formation: implications for engineered heart valve tissues. Biomaterials 27, 6083–6095.
Flanagan, T.C., Pandit, A., 2003. Living artificial heart valve alternatives: a review. Eur. Cells Mater. 6, 28–45.
Frisch-Fay, R., 1962. Flexible Bars. Butterworths, Washington, DC.
Gauvin, R., Guillemette, M., Dokmeci, M., Khademhosseini, A., 2011. Application of microtechnologies for the vascularization of engineered tissues. Vasc. Cell 3 (24), 1–7. (art. no. 24).
Gerosa, G., Ross, D.N., Brucke, P.E., Dziatkowiak, A., Mohammad, S., Norman, D., Davies, J., Sbarbati, A., Casarotto, D., Yankah, C., Barratt-Boyes, B., 1994. Aortic valve replacement with pulmonary homografts: early experience. J. Thorac. Cardiovasc. Surg. 107, 424–437.
Gloeckner, D.C., Billiar, K.L., Sacks, M.S., 1999. Effects of mechanical fatigue on the bending properties of the porcine bioprosthetic heart valve. ASAIO J. 45, 59–63.
Grashow, J.S., Sacks, M.S., Liao, J., Yoganathan, A.P., 2006a. Planar biaxial creep and stress relaxation of the mitral valve anterior leaflet. Ann. Biomed. Eng. 34, 1509–1518.
Grashow, J.S., Yoganathan, A.P., Sacks, M.S., 2006b. Biaixal stress-stretch behavior of the mitral valve anterior leaflet at physiologic strain rates. Ann. Biomed. Eng. 34, 315–325.
Guyton, A.C., 1976. Textbook of Medical Physiology. W.B. Saunders Company, Philadelphia.
Hasan, A., Memic, A., Annabi, N., Hossain, M., Paul, A., Dokmeci, M.R., Dehghani, F., Khademhosseini, A. Electrospun scaffolds for tissue engineering of vascular grafts. Acta Biomater, http://dx.doi.org/10.1016/j.actbio.2013.08.022, in press.
Hoerstrup, S.P., Sodian, R., Daebritz, S., Wang, J., Bacha, E.A., Martin, D.P., Moran, A.M., Guleserian, K.J., Sperling, J.S., Kaushal, S., Vacanti, J.P., Schoen, F.J., Mayer, J.E., 2000. Functional living trileaflet heart valves grown *in vitro*. Circulation 102, 44–49.
Holzapfel, G.A., Gasser, T.C., Ogden, R.W., 2000. A new constitutive framework for arterial wall mechanics and a comparative study of material models. J. Elast. 61, 1–48.
Isenberg, B.C., Williams, C., Tranquillo, R.T., 2006. Small-diameter artificial arteries engineered *in vitro*. Circ. Res. 98, 25–35.
Karimi, R., Zhu, T., Bouma, B.E., Mofrad, M.R.K., 2008. Estimation of nonlinear mechanical properties of vascular tissues via Elastography. Cardiovascular Engineering 8 (4), 191–202.
Kaazempur Mofrad, M.R., Abdul-Rahim, N.A., Karcher, H., Mack, P.J., Yap, B., Kamm, R.D., 2005. Exploring the molecular basis for mechanosensation, signal transduction, and cytoskeletal remodeling. Acta biomaterialia 1 (3), 281–293.
Khademhosseini, A., Vacanti, J.P., Langer, R., 2009. Progress in tissue engineering. Sci. Am 300 (5), 64–71.
Kim, A.K., Hasan, M.A., Lee, H.J., Cho, S.S., 2005. Characterization of submicron mechanical properties of Al-alloy foam using nanoindentation technique. Mater. Sci. Forum 475, 4199–4202.
Kuida, H., Lange, R.L., Brown, A.M., Hecht, H.H., 1961. Cardiovascular studies on normal calves. Am. J. Physiol. 200, 247–252.
Latremouille, C., Lintz, F., 2005. Anatomie du coeur. EMC - Cardiologie-Angeiologie 2, 231–251.
Lee, J.M., Courtman, D.W., Boughner, D.R., 1984. The glutaraldehyde-stabilized porcine aortic valve xenograft. I. Tensile viscoelastic properties of the fresh leaflet material. J. Biomed. Mater. Res. 18, 61–77.
Leeson-Dietrich, J., Boughner, D., Vesely, I., 1995. Porcine pulmonary and aortic valves: a comparison of their tensile viscoelastic properties at physiological strain rates. J. Heart Valve Dis. 4, 88–94.
Lewinsohn, A.D., Anssari-Benham, A., Lee, D.A., Taylor, P.M., Chester, A.H., Yacoub, M.H., Screen, H.R.C., 2011. Anisotropic strain transfer through the aortic valve and its relevance to the cellular mechanical environment. Proc. Inst. Mech. Eng. Part H: J. Eng. Med. 225, 821–830.
Lim, K.O., Boughner, D.R., 1976. The low-frequency dynamic viscoelastic properties of human aortic-valve tissue. Circ. Res. 39, 209–214.
Loftin, M.K.S., Chun, Y.W., Khademhosseini, A., Merryman, W.D., 2011. EMT-inducing biomaterials for heart valve engineering: taking cues from developmental biology. J. Cardiovasc. Trans. Res. 4, 658–671.
Martin, C., Pham, T., Sun, W., 2011. Significant differences in the material properties between aged human and porcine aortic tissues. Eur. J. Cardio-Thorac. Surg. 40, 28–34.
Martin, C., Sun, W., 2012. Biomechanical characterization of aortic valve tissue in humans and common animal models. J. Biomed. Mater. Res. A 100A, 1591–1599.
Mavrilas, D., Missirlis, Y., 1991. An approach to the optimization of preparation of bioprosthetic heart-valves. J. Biomech. 24, 331–339.
McAlpine, W.A., 1975. Heart and Coronary Arteries. Springer, Berlin, New York.
Merryman, W.D., Huang, H.Y.S., Schoen, F.J., Sacks, M.S., 2006. The effects of cellular contraction on aortic valve leaflet flexural stiffness. J. Biomech. 39, 88–96.
Mirnajafi, A., Raymer, J., Scott, M.J., Sacks, M.S., 2005. The effects of collagen fiber orientation on the flexural properties of pericardial heterograft biomaterials. Biomaterials 26, 795–804.
Mirnajafi, A., Raymer, J.M., McClure, L.R., Sacks, M.S., 2006. The flexural rigidity of the aortic valve leaflet in the commissural region. J. Biomech. 39, 2966–2973.
Misfeld, M., Sievers, H.H., 2007. Heart valve macro- and microstructure. Philos. Trans. R. Soc. B: Biol. Sci. 362, 1421–1436.
Missirlis, Y.F., 1973. *In Vitro* Studies of Human Aortic Valve Mechanics (Ph.D. thesis). Rice University, Houston, TX.
Missirlis, Y.F., Armeniades, C.D., 1976. Stress analysis of the aortic valve during diastole: important parameters. J. Biomech. 9, 477–480.
Nandy, S., Tarbell, J.M., 1987. Flush mounted hot film anemometer measurement of wall shear stress distal to a tri-leaflet valve for Newtonian and non-Newtonian blood analog fluids. Biorheology 24, 483–500.
Narine, K., Ing, E.C., Cornelissen, M., Desomer, F., Beele, H., Vanlangenhove, L., De Smet, S., Van Nooten, G., 2006. Readily available porcine aortic valve matrices for use in tissue valve engineering. Is cryopreservation an option? Cryobiology 53, 169–181.
Otto, C.M., 2001. Evaluation and management of chronic mitral regurgitation. N. Engl. J. Med. 345, 740–746.
Ragaert, K., De Somer, F., Somers, P., De Baere, I., Cardon, L., Degrieck, J., 2012. Flexural mechanical properties of porcine aortic heart valve leaflets. J. Mech. Behav. Biomed. Mater. 13, 78–84.
Reeves, J.T., Alexander, A.F., Grover, R.F., Will, D.H., 1962. Hemodynamics in normal cattle. Circ. Res. 10, 166–171.
Ross, D., Jackson, M., Davies, J., 1992. The pulmonary autograft – a permanent aortic valve. Eur. J. Cardio-Thorac. Surg. 6, 113–117.
Rousseau, E.P.M., Sauren, A.A.H.J., Hout, M.C.v., Steenhoven, A.A.v., 1983. Elastic and viscoelastic material behavior of fresh and glutaraldehyde-treated porcine aortic valve tissue. J. Biomech. 16, 339–348.
Sabbah, H.N., Hamid, M.S., Stein, P.D., 1985. Estimation of mechanical stresses on closed cusps of porcine bioprosthetic valves – effects of stiffening, focal calcium and focal thinning. Am. J. Cardiol. 55, 1091–1096.
Sabbah, H.N., Hamid, M.S., Stein, P.D., 1986. Mechanical stresses on closed cusps of porcine bioprosthetic valves – correlation with sites of calcification. Ann. Thorac. Surg. 42, 93–96.
Sacks, M.S., Merryman, W.D., Schmidt, D.E., 2009. On the biomechanics of heart valve function. J. Biomech. 42, 1804–1824.
Sacks, M.S., Smith, D.B., Hiester, E.D., 1998. The aortic valve microstructure: effects of transvalvular pressure. J. Biomed. Mater. Res. 41, 131–141.
Sacks, M.S., Yoganathan, A.P., 2007. Heart valve function: a biomechanical perspective. Philos. Trans. R. Soc. B: Biol. Sci. 362, 1369–1391.

Please cite this article as: Hasan, A., et al., Biomechanical properties of native and tissue engineered heart valve constructs. Journal of Biomechanics (2013), http://dx.doi.org/10.1016/j.jbiomech.2013.09.023

Sauren, A.A.H.J., Hout, M.C.v., Streenhoven, A.A.v., Veldpaus, F.E., Jansen, J.D., 1983. The mechanical properties of porcine aortic valve leaflets. J. Biomech. 16, 327–337.
Shinoka, T., Ma, P.X., Shum-Tim, D., Breuer, C.K., Cusick, R.A., Zund, G., Langer, R., Vacanti, J.P., Mayer Jr., J.E., 1996. Tissue-engineered heart valves: autologous valve leaflet replacement study in a lamb model. Circulation 94, II164–II168.
Simionescu, D.T., Chen, J., Jaeggli, M., Wang, B., Liao, J., 2012. Form follows function: advances in trilayered structure replication for aortic heart valve tissue engineering. J. Healthcare Eng. 3, 179–202.
Sodian, R., Hoerstrup, S.P., Sperling, J.S., Daebritz, S., Martin, D.P., Moran, A.M., Kim, B.S., Schoen, F.J., Vacanti, J.P., Mayer, J.E., 2000a. Early in vivo experience with tissue-engineered trileaflet heart valves. Circulation 102, 22–29.
Sodian, R., Hoerstrup, S.P., Sperling, J.S., Martin, D.P., Daebritz, S., Mayer Jr., J.E., Vacanti, J.P., 2000b. Evaluation of biodegradable, three-dimensional matrices for tissue engineering of heart valves. ASAIO J. 46, 107–110.
Stella, J.A., D'Amore, A., Wagner, W.R., Sacks, M.S., 2010. On the biomechanical function of scaffolds for engineering load-bearing soft tissues. Acta Biomater. 6, 2365–2381.
Stella, J.A., Liao, J., Sacks, M.S., 2007. Time-dependent biaxial mechanical behavior of the aortic heart valve leaflet. J. Biomech. 40, 3169–3177.
Stella, J.A., Sacks, M.S., 2007. On the biaxial mechanical properties of the layers of the aortic valve leaflet. J. Biomech. Eng.: Trans. ASME 129, 757–766.
Stradins, P., Lacis, R., Ozolanta, I., Purina, B., Ose, V., Feldmane, L., Kasyanov, V., 2004. Comparison of biomechanical and structural properties between human aortic and pulmonary valve. Eur. J. Cardio-Thorac. Surg. 26, 634–639.
Sun, W., Sacks, M.S., 2005. Finite element implementation of a generalized Fung-elastic constitutive model for planar soft tissues. Biomech. Model. Mechanobiol. 4, 190–199.
Sun, W., Sacks, M.S., Sellaro, T.L., Slaughter, W.S., Scott, M.J., 2003. Biaxial mechanical response of bioprosthetic heart valve biomaterials to high in-plane shear. J. Biomech. Eng: Trans. ASME 125, 372–380.
Sutherland, F.W.H., Perry, T.E., Yu, Y., Sherwood, M.C., Rabkin, E., Masuda, Y., Garcia, G.A., McLellan, D.L., Engelmayr, G.C., Sacks, M.S., Schoen, F.J., Mayer, J.E., 2005. From stem cells to viable autologous semilunar heart valve. Circulation 111, 2783–2791.
Tan, A.J., Holt, D.L., 1976. The effects of sterilization and storage treatments on the stress–strain behaviour. Ann. Thorac. Surg. 22, 188–194.
Thubrikar, M., Piepgrass, W.C., Deck, J.D., Nolan, S.P., 1980. Stresses of natural *versus* prosthetic aortic valve leaflets *in vivo*. Ann. Thorac. Surg. 30, 230–239.
Vesely, I., 1998. The role of elastin in aortic valve mechanics. J. Biomech. 31, 115–123.
Vesely, I., 2005. Heart valve tissue engineering. Circ. Res. 97, 743–755.
Vesely, I., Boughner, D., 1989. Analysis of the bending behavior of porcine xenograft leaflets and of natural aortic-valve material – bending stiffness, neutral axis and shear measurements. J. Biomech. 22, 655–671.
Vesely, I., Noseworthy, R., 1992. Micromechanics of the fibrosa and the ventricularis in aortic valve leaflets. J. Biomech. 25, 101–113.
Wang, X., Li, X., Yost, M.J., 2005. Microtensile testing of collagen fibril for cardiovascular tissue engineering. J. Biomed. Mater. Res. A 74A, 263–268.
Weiler, M., Hwai Yap, C., Balachandran, K., Padala, M., Yoganathan, A.P., 2011. Regional analysis of dynamic deformation characteristics of native aortic valve leaflets. J. Biomech. 44, 1459–1465.
Weinberg, E.J., Kaazempur-Mofrad, M.R., 2006. A large-strain finite element formulation for biological tissues with application to mitral valve leaflet tissue mechanics. J. Biomech. 39, 1557–1561.
Weinberg, E.J., Kaazempur Mofrad, M.R., 2007a. A finite shell element for heart mitral valve leaflet mechanics, with large deformations and 3D constitutive material model. J. Biomech. 40, 705–711.
Weinberg, E.J., Kaazempur Mofrad, M.R., 2007b. Transient, three-dimensional, multiscale simulations of the human aortic valve. Cardiovasc. Eng. 7, 140–155.
Weinberg, E.J., Kaazempur Mofrad, M.R., 2008. A multiscale computational comparison of the bicuspid and tricuspid aortic valves in relation to calcific aortic stenosis. J. Biomech. 41, 3482–3487.
Weinberg, E.J., Mofrad, M.R.K., 2005. On the constitutive models for heart valve leaflet mechanics. Cardiovasc. Eng.: Int. J. 5, 37–44.
Weinberg, E.J., Shahmirzadi, D., Mofrad, M.R.K., 2010. On the multiscale modeling of heart valve biomechanics in health and disease. Biomech. Model. Mechanobiol. 9, 373–387.
Weston, M.W., LaBorde, D.V., Yoganathan, A.P., 1999. Estimation of the shear stress on the surface of an aortic valve leaflet. Ann. Biomed. Eng. 27, 572–579.
Xu, F., Lu, T., 2011. Introduction to Skin Biothermomechanics and Thermal Pain. Springer, Heidelberg, Dordrecht, London, New York.
Yacoub, M.H., Takkenberg, J.J.M., 2005. Will heart valve tissue engineering change the world? Nat. Clin. Pract. Cardiovasc. Med. 2, 60–61.
Yamada, H., 1973. Tensile properties of human cardiac valves. In: Evans, G.F. (Ed.), Strength of Biological Materials. Krieger, New York, p. 109. (Chapter 4.1.4).

Please cite this article as: Hasan, A., et al., Biomechanical properties of native and tissue engineered heart valve constructs. Journal of Biomechanics (2013), http://dx.doi.org/10.1016/j.jbiomech.2013.09.023